Available online at www.sciencedirect.com
ScienceDirect
Journal of Magnetic Resonance 185 (2007) 221–229
JMR Journal of Magnetic Resonance
www.elsevier.com/locate/jmr

^{13}C–^{1}H HSQC experiment of probe molecules aligned in thermotropic liquid crystals: Sensitivity and resolution enhancement in the indirect dimension

Bikash Baishya [a,b], Raghav G. Mavinkurve [c], N. Suryaprakash [b,*]

[a] Solid State and Structural Chemistry Unit, Indian Institute of Science, Bangalore 560 012, India
[b] NMR Research Centre, Indian Institute of Science, Bangalore 560 012, India
[c] Department of Physics, Indian Institute of Science, Bangalore 560 012, India

Received 10 October 2006; revised 24 December 2006
Available online 30 December 2006

Abstract

The spectra of molecules oriented in liquid crystalline media are dominated by partially averaged dipolar couplings. In the ^{13}C–^{1}H HSQC, due to the inefficient hetero-nuclear dipolar decoupling in the indirect dimension, normally carried out by using a π pulse, there is a considerable loss of resolution. Furthermore, in such strongly orienting media the ^{1}H–^{1}H and ^{13}C–^{1}H dipolar couplings leads to fast dephasing of transverse magnetization causing inefficient polarization transfer and hence the loss of sensitivity in the indirect dimension. In this study we have carried out ^{13}C–^{1}H HSQC experiment with efficient polarization transfer from ^{1}H to ^{13}C for molecules aligned in liquid crystalline media. The homonuclear dipolar decoupling using FFLG during the INEPT transfer delays and also during evolution period combined with the π pulse heteronuclear decoupling in the t_1 period has been applied. The studies showed a significant reduction in partially averaged dipolar couplings and thereby enhancement in the resolution and sensitivity in the indirect dimension. This has been demonstrated on pyridazine and pyrimidine oriented in the liquid crystal. The two closely resonating carbons in pyrimidine are better resolved in the present study compared to the earlier work [H.S. Vinay Deepak, Anu Joy, N. Suryaprakash, Determination of natural abundance ^{15}N–^{1}H and ^{13}C–^{1}H dipolar couplings of molecules in a strongly orienting media using two-dimensional inverse experiments, Magn. Reson. Chem. 44 (2006) 553–565].

Keywords: HSQC spectrum; FSLG; FFLG; INEPTRD

1. Introduction

NMR spectra of molecules oriented in liquid crystals provide homo and heteronuclear dipolar couplings and thereby the geometry of the molecules. Several inequivalent dilute spins such as ^{13}C and ^{15}N coupled to protons form different coupled spin systems in their natural abundance and appear as satellites in the proton spectra. The identification of spectra corresponding to each coupled spin system is a prerequisite for the determination of dipolar couplings and it is a formidable task. We have shown earlier, using two-dimensional ^{15}N–^{1}H and ^{13}C–^{1}H Heteronuclear single quantum coherence (HSQC) and Heteronuclear multiple quantum coherence (HMQC) experiments, that selective detection of spectra of each rare spin coupled to protons is possible [1–3]. The dipolar decoupling has been carried out in the HSQC/HMQC experiments during the evolution period to obtain ^{13}C chemical shifts in the oriented phase. The normal spectrum dominated by proton–proton (D_{HH}'s) and proton–carbon (D_{CH}'s) dipolar couplings is obtained in the direct dimension. The spectra are obtained without any phase distortion. The cross section of the spectrum taken at the chemical shift positions of different carbons in the indirect dimension provides the spectrum of the particular carbon coupled to protons, the analysis of which provided

* Corresponding author. Fax: +91 80 2360 1550.
E-mail address: nsp@sif.iisc.ernet.in (N. Suryaprakash).

1090-7807/$ - see front matter © 2007 Elsevier Inc. All rights reserved.
doi:10.1016/j.jmr.2006.12.014

both proton–proton and proton–carbon dipolar couplings. Thus the simultaneous determination of D_{HH}'s and also D_{CH}'s in the natural abundance of rare spin has been made. Several advantages of this method have already been discussed in our earlier publications [1,2]. In all the earlier studies the dipolar decoupling has been achieved in the indirect dimension by the use of π pulse in the middle of the evolution period. Since the homo and heteronuclear terms of the dipolar Hamiltonian do not commute, and the spin systems in liquid crystalline media are generally strongly coupled, this decoupling is inefficient. This gives rise to many unresolved transitions leading to large spread of contours in F1 dimension. This was seen in our earlier study [1] on pyrimidine oriented in the liquid crystals where the two closely resonating carbons were not resolved. This is also evident from the spread of the contours in the indirect dimension of the HSQC experiment. Furthermore, homonuclear and heteronuclear D_{IJ}'s also results in spin diffusion type magnetization transfer during insensitive nuclei enhanced polarization transfer (INEPT) and hence loss of sensitivity. Therefore, we have carried out studies to explore the good heteronuclear decoupling sequence combined with homonuclear decoupling in the t_1 dimension for better resolution and sensitivity. The multiple pulse techniques [4] are a well-known method for homonuclear decoupling. However, these experiments are technically demanding.

The use of off resonance Lee–Goldburg (LG) decoupling [5] is another way of removing homonuclear dipolar couplings which is widely employed in solid state studies and is easy to implement. There are many LG sequences reported in the literature such as, flip flop Lee–Goldburg (FFLG) [6], frequency switched Lee–Goldburg (FSLG) [7,8], phase modulated Lee–Goldburg (PMLG) [9], Lee–Goldburg cross polarization (LGCP) [10]. These LG sequences are designed to remove homonuclear dipolar couplings and find extensive applications in the separated local field (SLF) experiments. These sequences are referred to as PISEMA (polarization inversion spin exchange at magic angle) [11], TANSEMA (time averaged nutation spin exchange at magic angle) [12] PITANSEMA (polarization inversion time averaged nutation spin exchange at magic angle) [13], PITANSEMA-MAS (polarization inversion time averaged nutation spin exchange at magic angle under magic angle spinning) [14]. A review highlights several applications of PISEMA sequence [15].

As far as the ^{13}C NMR spectra of pure thermotropic liquid crystals is concerned, the studies have been carried out to explore the best homonuclear and heteronuclear decoupling sequence and their merits and demerits have been discussed [16–19]. However, there is no such systematic study for the probe molecules aligned in the liquid crystalline media, although in a study on the mono and disubstituted fluorinated benzenes aligned in the liquid crystals a two-dimensional proton-detected local field (PDLF) experiment has been carried out [20], using the PMLG sequence to suppress the proton–proton dipolar couplings in the indirect dimension, allowing the evolution of fluorine and proton dipolar couplings. The normal proton spectrum with ^1H–^1H and ^{19}F–^1H dipolar couplings has been detected in the direct dimension. The method has been exploited to utilize the proton–fluorine dipolar couplings to aid the analysis of the complex proton spectra.

In the present study we have utilised the Lee–Goldburg decoupling with frequency switching. Though it is referred to as FSLG in the literature, in a review, it has been pointed out that effect of either phase modulation or frequency modulation using LG, the net result is the flip flop of the effective field direction and ideally it should be called FFLG [15]. We have employed FFLG sequence during the t_1 period and also during the INEPT transfer and back transfer delays of the HSQC experiment. This resulted in the removal of the partially averaged dipolar couplings to a significant extent and the polarization transfer was under pure heteronuclear dipolar couplings and *J*-couplings. This is combined with π pulse heteronuclear decoupling in the t_1 period. A significant enhancement in the resolution and the sensitivity in t_1 dimension could be obtained. The results of the study on the two systems, pyrimidine and pyridazine aligned in liquid crystals, are reported.

2. Experimental

The chemical structure and numbering of pyrimidine and pyridazine are shown in Fig. 1. The liquid crystal phase IV was obtained from MERCK. The solute molecules pyrimidine and pyridazine obtained from Sigma–Aldrich were used without further purification. Approximately five per cent by weight solutions of pyridazine and pyrimidine in phase IV were prepared. All the spectra were recorded on a Bruker AV-500 NMR spectrometer with field strength of 11.7 T operating at frequencies of 500.13 and 125.77 MHz for ^1H and ^{13}C nuclei, respectively, using 5 mm QXI probes. The temperature was maintained at 300 K by a Bruker BVT-3000 temperature regulating system. The samples were not spun during acquisition. The homogeneous solutions of these samples gave a line width of less than 4 Hz for both pyrimidine and pyridazine solutions in the ^1H spectra.

The pulse sequence used for the INEPT technique with refocusing for decoupled spectra (INEPTRD) [21] and the HSQC experiment is given in Fig. 2a and b, respectively. The LG durations were 62 μs which were implemented as a function of incremental delays. This puts a limit on the total spectral width in F1 dimension. For HSQC the echo and 'anti-echo' mode was followed with gradient selection.

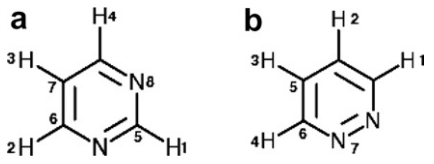

Fig. 1. The chemical structure and the numbering of interacting spins in (a) pyrimidine and (b) pyridazine.

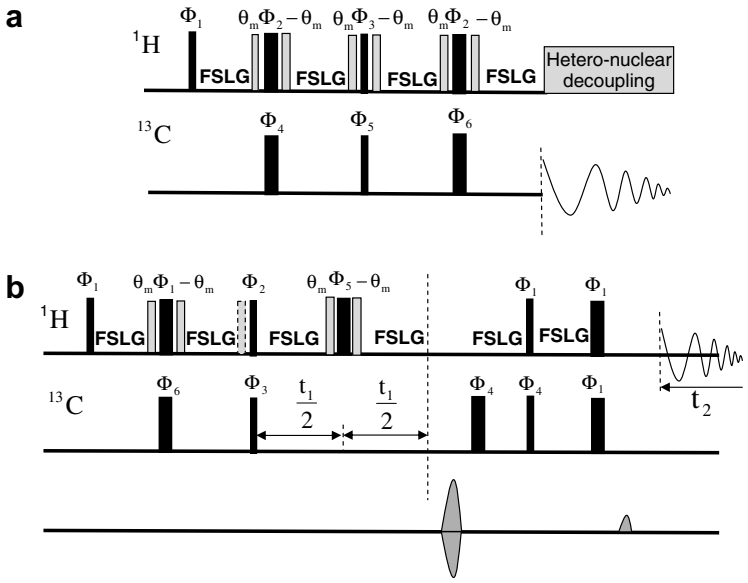

Fig. 2. (a) The INEPTRD pulse sequence with FFLG during polarization transfer, the phases of the pulses are $\varphi_1 = 8(0)\ 8(-0)$, $\varphi_2 = 02$, $\varphi_3 = 1133$, $\varphi_4 = 02$, $\varphi_5 = 0000111122223333$, $\varphi_6 = 02021313$, Receiver phase = 00221133, FFLG phase during INEPT +X and −X and θ_m (phase) = 0; (b) HSQC pulse sequence with FFLG during t_1 evolution and also during polarization transfer and back transfer delays, the phases of the pulses are: $\varphi_1 = 0$ $\varphi_2 = 1$, $\varphi_3 = 02$, $\varphi_4 = 00002222$, $\varphi_5 = 0022$, $\varphi_6 = 0$, Receiver phase = 02022020, FFLG phases +x during $t_1/2$ increments and during INEPT +X and −X and θ_m (phase) = 0. The LG decoupling power is 13 kHz. The frequency offset is 8600 Hz. During acquisition period, the SPINAL decoupling power of 10.8 kHz was used.

For all the ^{13}C–^{1}H HSQC spectra of pyridazine solution a dataset consisting of 3K and 80 points in F2 and F1 dimensions, respectively, were chosen. It may be pointed out that more number of t_1 increments could have given better resolution. However, this leads to significantly larger RF power for a longer duration. This was avoided due to probe constraints. Although the maximum power requirement is limited by the probe, which in the present case is 13 kHz, the minimum required is about three times the largest dipolar coupling. The largest dipolar coupling observed in the molecules of our study is less than 1.5 kHz. Thus the maximum 13 kHz rf power used in the LG decoupling was sufficient for good decoupling. The number of scans was 64 for each t_1 increment. Relaxation delay was 3.5 s. As far as the delays for transfer of polarization during INEPT is concerned, it is not straightforward unlike in isotropic systems where it depends on J_{CH} and the same can be easily estimated. In oriented systems the efficiency of the polarization transfer depends on T_{CH}, where T_{CH} corresponds to $J_{CH} + 2D_{CH}$. The magnitudes of the dipolar couplings between different interacting spins are not the same and thus the evolution of the magnetization for different groups like CH, CH_2 and CH_3 are different. Also the dipolar couplings differ for each sample depending on the molecular order. However, the molecules chosen for our study has only CH groups. Even in this situation the dipolar couplings of each inequivalent carbon to different protons are different. The variation of the intensity of the peaks with the tau delay is discussed in earlier publication [3]. Therefore, the delays need to be optimized for each sample by carrying out several experiments. For the present study, a good spectrum with reasonable intensities for most of the transitions was obtained for the delay of 1.04 ms. This delay gave the maximum intensity for HSQC with the π pulse and also for the experiments involving FFLG. This value was kept constant in all the 2D experiments concerning this molecule. The time domain data was zero filled to 8k and 1k points, processed with unshifted and shifted squared sine bell window functions, in the direct and indirect dimensions, respectively. The F1 dimension was linear predicted to 512 data points. The spectrum is displayed in magnitude mode with a digital resolution of 0.9 and 7.7 Hz in the direct and indirect dimensions, respectively.

For all the 2D ^{13}C–^{1}H experiments on pyrimidine, a dataset consisting of 4k and 96 points in F2 and F1 dimensions, respectively, were chosen. The number of scans was 96 for each t_1 increment. The optimized τ_1 delay for polarization was 1312 μs and the relaxation delay of 3.5 s was kept constant in all the experiments. The time domain data was zero filled to 8k and 1k points, processed with unshifted and shifted squared sine bell window functions, in the direct and indirect dimensions, respectively. The F1 dimension was linear predicted to 512 data points. The spectrum is displayed in magnitude mode with a digital resolution of 0.8 and 8.1 Hz in the direct and indirect dimensions, respectively.

3. Results and discussion

The TPPM (two pulse phase modulation) [22], SPINAL-64 (small phase incremental alternation, with 64 steps) [19]

broadband decoupling and π pulse decoupling were explored in the t_1 dimension of ^{13}C–^{1}H HSQC experiment of pyrimidine and pyridazine solutions. The HSQC spectra for pyrimidine solution are shown in Fig. 3a–c along with their corresponding projections on the F2 axis. The spread of the contours along the F1 dimension implies that the heteronuclear dipolar couplings are not completely removed by these sequences. However, from the F2 projections one can see that the HSQC spectra with SPINAL-64 sequence (Fig. 3a) has the enhanced signal intensity for many peaks compared to TPPM and π pulse decoupling (Fig. 3b and c). The similar observations were also made on the pyridazine solution whose spectra are not shown. Thus the combined Homonuclear and heteronuclear decoupling was explored in the indirect dimension to improve the sensitivity and resolution.

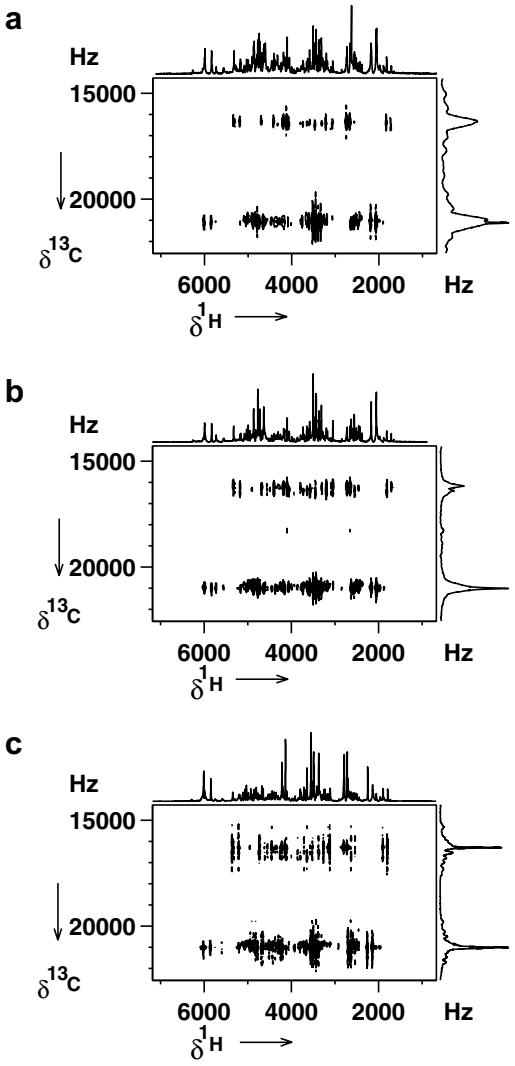

Fig. 3. ^{13}C–^{1}H HSQC spectrum of pyrimidine oriented in phase IV with different heteronuclear decoupling sequences along t_1 dimension; (a) SPINAL-64 decoupling with an rf power of 10.8 kHz, (b) TPPM decoupling with an rf power of 10.8 kHz and (c) with π pulse decoupling. The corresponding projections on F1 and F2 are also given.

In a recent study on the weakly aligned molecules it has been shown that application of the phase modulated Lee–Goldburg sequence in the INEPT periods increased the efficiency of the magnetization transfer [23] and removed the effects of residual dipolar truncation. This led to a significant sensitivity increase and the method aided the detection of long-range partially averaged heteronuclear dipolar couplings on enriched biological samples. We explored the possibility of incorporating similar LG decoupling during the INEPT transfer and back transfer delays of the HSQC sequence. However, it is not possible to translate that pulse sequence for the present study. This is because in weakly aligned systems the dipolar couplings are small because of low order parameter. Furthermore, the PMLG sequence scales heteronuclear dipolar couplings. Therefore, the pulse sequence provided enhanced sensitivity and resolution. On the other hand in thermotropic liquid crystals the order parameter (10^{-1}) is several orders of magnitude larger than the weakly aligning medium (10^{-4}). The spectra are not first order. Thus designing a pulse sequence for removal of the strong dipolar couplings is more challenging. In addition, our aim is to carry out the study at the natural abundance of ^{13}C, where the sensitivity is an important factor.

In our ^{13}C–^{1}H HSQC experiments, the homonuclear decoupling was achieved by using FFLG. As it is not possible for the simultaneous application of decoupling schemes like SPINAL-64, TPPM, etc., with FFLG, the heteronuclear decoupling was achieved by applying π pulse in the middle of t_1 period.

The use of FFLG requires the optimization of the off-resonance frequency list. To save experimental time, this was carried out on one-dimensional ^{13}C signal using INEPTRD pulse sequence [21]. The FFLG decoupling power used during INEPT period was 13 kHz. In general, the optimization of FFLG is obtained by monitoring the scaling factor on the chemical shift of protons which is 0.58. However, in the present case, since the indirect dimension was ^{13}C, whose anisotropic chemical shifts are unknown, the optimization was carried out by monitoring the signal intensity in INEPTRD experiment. The optimized frequency list gave the drastic enhancement in the signal intensity for both pyrimidine and pyridazine solutions (figures not shown). The efficiency of the polarization transfer is such that the intensities of the liquid crystal carbons also started building up.

With the optimized frequency list, FFLG was initially applied only in the indirect dimension to ascertain the improvement in the sensitivity and resolution, if any. The π pulse was also applied in the middle of the t_1 dimension. The spectra of two experiments on pyrimidine solution, viz., (a) with heteronuclear decoupling (with only π pulse in the middle of t_1 period) and (b) with both heteronuclear and homonuclear decoupling (the π pulse and FFLG) are compared in Fig. 4a and b. The expanded plots of the particular region of Fig. 4a and b are shown in Fig. 4c and d, respectively. It is clear that the effects of partially averaged

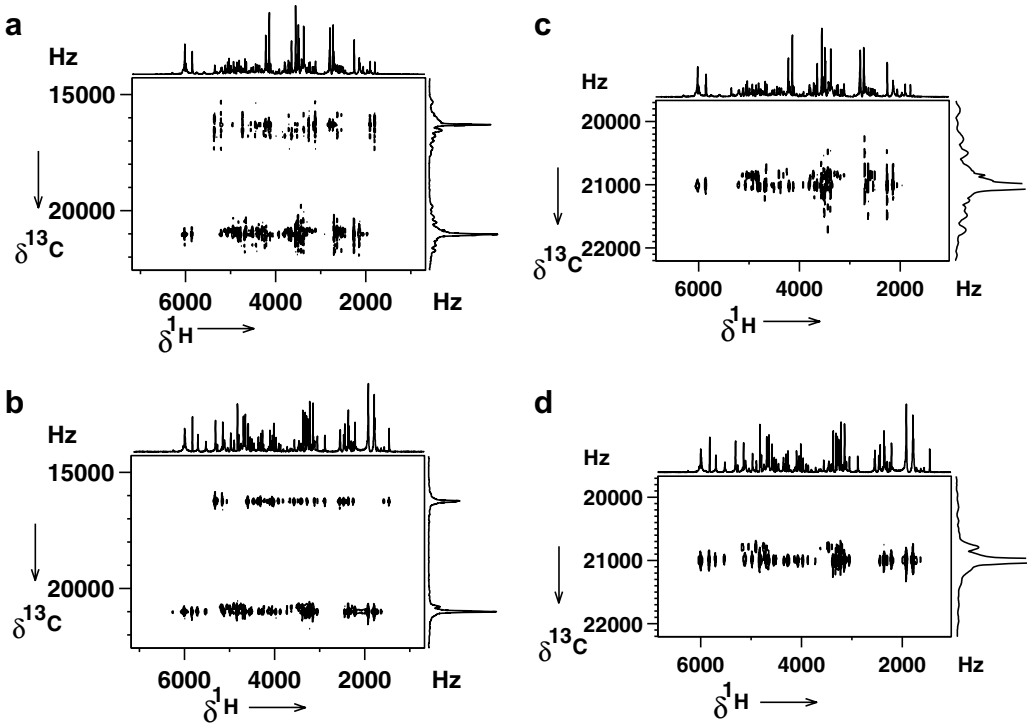

Fig. 4. ^{13}C–^{1}H HSQC spectrum of pyrimidine oriented in phase IV, (a) only with heteronuclear decoupling using π pulse during t_1 period, (b) with combined homonuclear decoupling using FFLG and heteronuclear decoupling using π pulse during the t_1 period, (c) the expansion of spectrum between the region 20,000 and 22,000 Hz of (a) and (d) the expansion of spectrum between the region 20,000 and 22,000 Hz of (b).

dipolar couplings are dominating in the experiment involving only heteronuclear decoupling (Fig. 4a). On the other hand, they are removed substantially in the experiment involving both homo and heteronuclear decoupling (Fig. 4b). The spread of the contours in F1 dimension in Fig. 4b is therefore reduced substantially. From Fig. 4c and d, one can see that the carbons numbered 5 and 6 are better resolved. Also the projection on F2 axis of Fig. 4b shows the enhanced intensity of several peaks. Experiments on pyridazine solution also gave similar results, whose spectra are not shown.

With this improvement in the sensitivity, the FFLG was then incorporated in the polarization transfer and back transfer periods of the above experiment. The HSQC spectrum of pyrimidine solution without any FFLG and the corresponding spectrum with FFLG during both INEPT and t_1 periods, is compared in Fig. 5a and b, respectively. The expanded plots of the particular region of Fig. 5a and b are shown in Fig. 5c and d, respectively. The F1 dimension spread of contours in Fig. 5b is drastically reduced compared to Fig. 5a, indicating that the effect of partially averaged dipolar couplings is substantially removed. This is also evident from the corresponding projections on the F1 axis. One can see from Fig. 5b, the carbons numbered 5 and 6 are better resolved compared to earlier experiments (Fig. 4a–d). The significant enhancement in the sensitivity can also be seen from the projections on the F2 axis. Some of the transitions that are not seen in F2 projections in Fig. 5a are seen in Fig. 5b. However, it may be mentioned that the F1 projections could be misleading. Therefore, for comparing the sensitivity of the experiments, the three different F2 slices, at the ^{13}C chemical shift positions of carbons numbered seven, five and six were chosen. These are shown in Fig. 6d–f. The corresponding plots of Fig 5a are shown in Fig. 6a–c. The advantage of the pulse sequence is evident that many peaks which are very weak in Fig. 6a–c are seen with enhanced intensity in Fig. 6d–f. However, comparison of Fig. 6b and e reveals that there are more transitions in Fig. 6B. This is because the slice was selected from carbon 5, which is very close to carbon 6 and is not precise. Furthermore, the Fig. 6b corresponds to spectrum of carbon numbered 5, coupled to protons.

The experiments were also carried out on pyridazine solution. Fig. 7a is the HSQC spectrum with FFLG during both INEPT and t_1 periods, and with π pulse in the middle of t_1 period. Fig. 7b is the HSQC experiment with only π pulse decoupling during the t_1. One can see drastic reduction in the spread of the contours along F1 dimension and enhanced sensitivity in Fig. 7a. Comparison of the slices of the rows selected at two ^{13}C chemical shifts positions in Fig. 7a and the slices of corresponding slices in Fig. 7b revealed the enhancement in resolution and sensitivity. Thus the studies on both the molecules indicate that even in the strongly oriented media, the additional use of FFLG in t_1 dimension and during INEPT delays of HSQC experiment provides spectra with enhanced sensitivity and resolution.

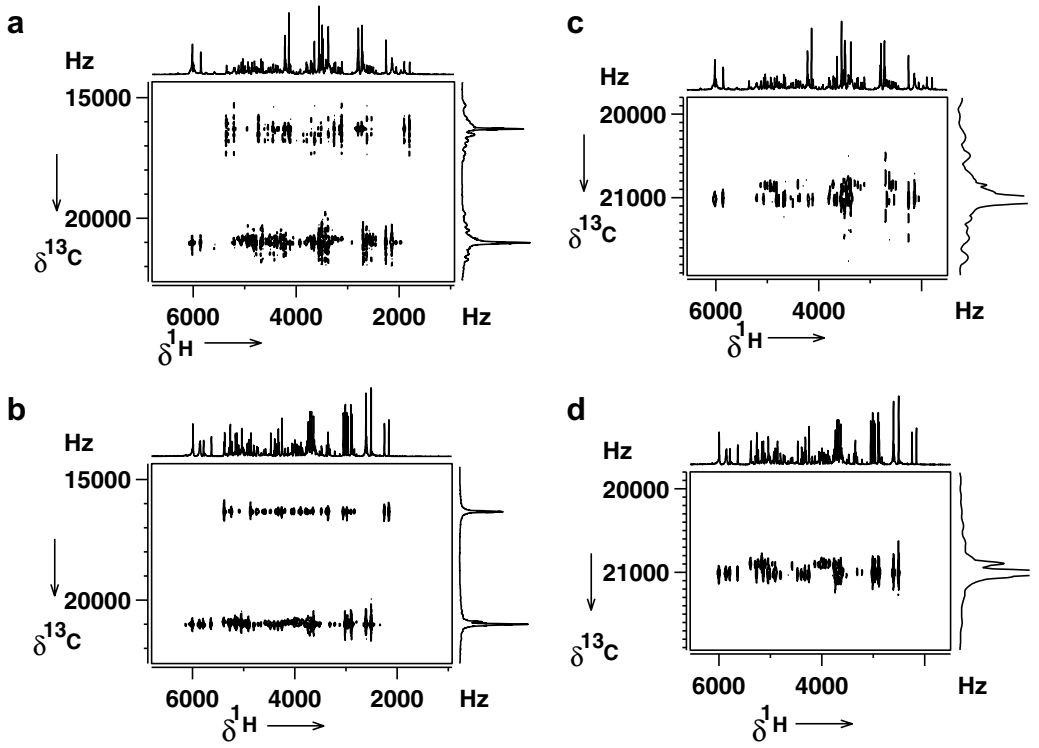

Fig. 5. The ^{13}C–^{1}H HSQC spectrum of pyrimidine in phase IV, (a) with only π pulse heteronuclear decoupling during evolution, (b) with the FFLG both during INEPT transfer delays and also during evolution period and with π pulse decoupling during the middle of t_1 dimension, (c) the expansion of spectrum between the region 20,500 and 21,500 Hz of (a) and (d) the expansion of spectrum between the region 20,500 and 21,500 Hz of (b).

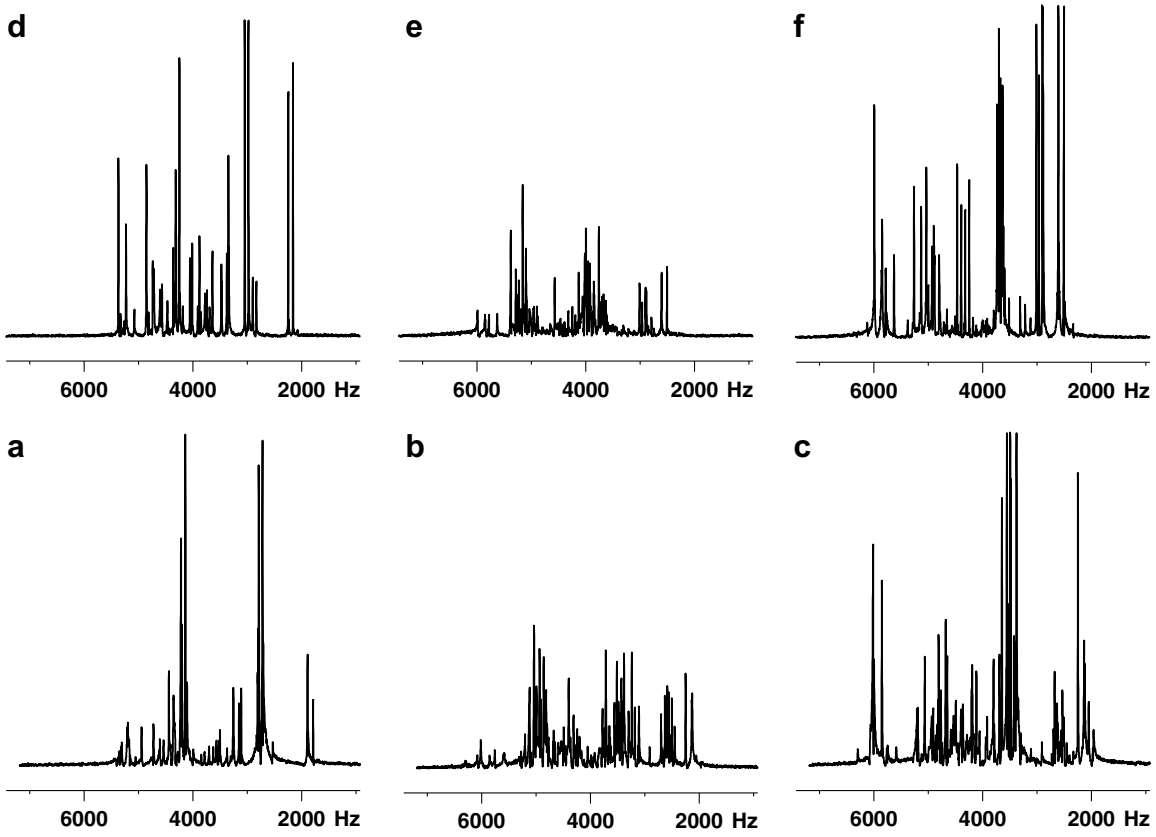

Fig. 6. (a–c) Slices taken at ^{13}C chemical shift positions of carbons numbered 7, 5 and 6, respectively, of Fig. 5a; (d–f) slices of the corresponding rows of Fig. 5b.

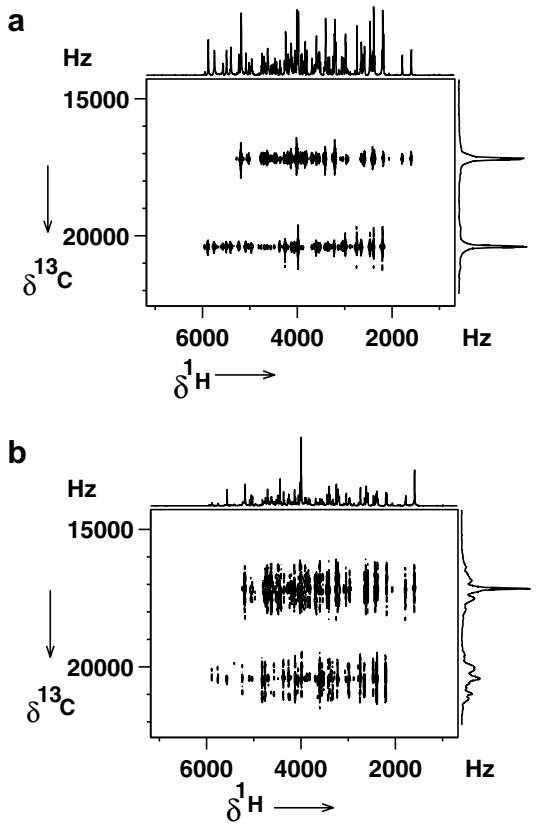

Fig. 7. The ^{13}C–^{1}H HSQC spectrum of pyridazine in phase IV; (a) with the FFLG both during INEPT transfer delays and also during evolution period and with π pulse decoupling during the middle of t_1 dimension; (b) with only π pulse heteronuclear decoupling during evolution.

There are several homonuclear decoupling sequences available in the literature. Studies are in progress to explore other sequences.

It may be worthwhile to mention that it is difficult to quantify the resolution and sensitivity enhancement as the spread of the contours depends on the strength of the dipolar couplings, which depends on molecular order. These parameters differ for different samples oriented in different liquid crystals. However, in the present study, one can see that the spread of the contours reduced by an order of magnitude. For example, in the normal HSQC sequence, the spread of the contours was around 1300 Hz in pyrimidine and it reduced to around 200 Hz with the present experiment for the upfield carbon. To demonstrate the use of present pulse sequence, the HSQC cross sections were analysed and compared with the parameters obtained by the ^{13}C satellite spectral analysis. The three five spin spectra of the type ABB′CX, ABCDX and ABB′CX in pyrimidine corresponding to carbons numbered 5, 6 and 7, respectively, and the two five spin spectra of the type ABCDX for two inequivalent carbons in pyridazine are required to be analysed. The iterative analyses of the spectra were carried out as discussed in the earlier communication [1]. The derived spectral parameters are given in Tables 1 and 2. The carbon 5 is directly bonded to two nitrogens and gave broad lines, in the satellites and also in HSQC cross section. The errors of the derived spectral parameters for this carbon were larger compared to spectra of other carbons. Hence this data is not reported in the table. However, for the analyses of the spectra for the remaining two carbons of pyrimidine and for both the spectra in pyridazine, the present study gave better spectrum and the number of transitions that could be assigned using HSQC cross sections is more than that from the ^{13}C satellite spectral analysis. Therefore, the determination of the spectral parameters using present HSQC experiment is likely to be more precise.

Table 1
The spectral parameters in pyrimidine oriented in the liquid crystal solvent phase IV obtained by the analyses of the ^{13}C satellites and ^{13}C–^{1}H HSQC spectra

For the ^{13}C isotopomer C6			For the ^{13}C isotopomers C5 and C7		
Parameter	^{13}C satellites	^{13}C–^{1}H HSQC cross section[a]	Parameter	^{13}C satellites	^{13}C–^{1}H HSQC cross section[a]
D_{12}	−64.63	−68.79	D_{12}	−57.806	−69.39
D_{13}	−35.06	−34.76	D_{13}	−37.221	−35.44
D_{14}	−64.26	−68.49	D_{15}	−598.67	
D_{16}	−27.08	−27.042	D_{17}	−17.15	−20.67
D_{23}	−343.40	−387.481	D_{23}	−328.89	−387.56
D_{24}	−75.98	−89.076	D_{24}	−70.87	−89.33
D_{26}	−37.66	−60.768	D_{25}	−45.61	
D_{34}	−323.348	−387.481	D_{27}	−144.87	−177.03
D_{36}	−97.44	−116.034	D_{35}	−27.46	
D_{46}	−973.66	−1173.489	D_{37}	−600.85	−710.89
$\nu_1 - \nu_2$	−262.2	−239.7	$\nu_1 - \nu_2$	−259.2	−239.7
$\nu_1 - \nu_3$	−952.7	−930.0	$\nu_1 - \nu_3$	−964.4	−930.0
$\nu_1 - \nu_4$	−263.6	−240.9			
Number of line assigned	20	32		19	28
RMS	1.9	1.26		1.69	1.8

The maximum error of the HH dipolar coupling is 0.1 Hz and CH coupling is 1.5 Hz.
[a] The parameters were derived from the spectra recorded at different times.

Table 2
The spectral parameters in pyridazine oriented in the liquid crystal solvent phase IV obtained by the analyses of the ^{13}C satellites and ^{13}C–^{1}H HSQC spectra

For the isotopomer C5			For the isotopomer C6		
Parameter	Derived by the analysis of ^{13}C satellites	Derived from ^{13}C–^{1}H HSQC spectrum	Parameter	Derived by the analysis of ^{13}C satellites	Derived from ^{13}C–^{1}H HSQC spectrum
D_{12}	−320.01	−318.56	D_{12}	−322.65	−318.33
D_{13}	−77.03	−75.77	D_{13}	−75.60	−77.61
D_{14}	−60.35	−59.67	D_{14}	−60.34	−61.02
D_{15}	−143.56	−141.80	D_{16}	−1220.63	−1223.39
D_{23}	−407.73	−405.71	D_{23}	−408.26	−406.64
D_{24}	−77.42	−78.59	D_{24}	−80.27	−77.50
D_{25}	−965.10	−964.43	D_{26}	−120.18	−113.92
D_{34}	−319.52	−319.83	D_{34}	−319.94	−318.86
D_{35}	−149.81	−154.76	D_{36}	−36.06	−38.33
D_{45}	−39.59	−36.54	D_{46}	−32.73	−34.44
$\nu_1 - \nu_2$	932.3 ± 0.45		$\nu_1 - \nu_2$	937.1 ± 1.163	927.59
$\nu_1 - \nu_3$	941.3 ± 0.66		$\nu_1 - \nu_3$	928.3 ± 1.25	931.26
$\nu_1 - \nu_4$	−0.172 ± 0.51		$\nu_1 - \nu_4$	7.269 ± 1.59	−2.48
Number of lines assigned	24	41	$\nu_5 - \nu_6$	25	53
RMS error	0.53	1.8		1.5	2.2

4. Conclusions

Systematic studies have been carried out to determine a suitable sequence for efficient heteronuclear decoupling of probe molecules in liquid crystalline media. The SPINAL-64 sequence is shown to provide good decoupling. The application of pulse sequence, incorporating FFLG during INEPT and t_1 periods and with π pulse during t_1 period of HSQC experiment, to probe molecules aligned in the strongly orienting media reduced the effects of partially averaged dipolar couplings and gave considerable enhancement in the signal sensitivity and resolution in the indirect dimension. The significant enhancement in the sensitivity is seen in the direct dimension also. Further work in this direction for the application of these sequences to more complex molecules to determine the structure and also to get the heteronuclear correlation in static liquid crystal samples is in progress and will be published elsewhere.

Acknowledgments

B.B. thanks Suresh kumar Vasa for discussions. N.S. gratefully acknowledges the financial support by Department of Science and Technology, New Delhi, for the research Grant SR/S1/PC-13/2004.

References

[1] H.S. Vinay Deepak, Anu Joy, N. Suryaprakash, Determination of natural abundance ^{15}N–^{1}H and ^{13}C–^{1}H dipolar couplings of molecules in a strongly orienting media using two-dimensional inverse experiments, Magn. Reson. Chem. 44 (2006) 553–565.
[2] S. Vivekanandan, N. Suryaprakash, Novel method of estimating proton–proton dipolar couplings to aid the analyses of NMR spectra of oriented molecules using two-dimensional inverse experiment, Chem. Phys. Lett. 338 (2001) 247.
[3] J.W. Emsley, D. Merlet, K.J. Smith, N. Suryaprakash, Selective detection of proton spectra of molecules containing rare spins at natural abundance in liquid crystalline samples, J. Magn. Reson. 154 (2002) 303.
[4] J.S. Waugh, L.M. Huber, U. Haeberlen, Approach to high resolution NMR in solids, Phys. Rev. Lett. 20 (1968) 180.
[5] M. Lee, W.I. Goldburg, Nuclear Magnetic Resonance line narrowing by a rotating RF field, Phys. Rev. A 140 (1965) 1261.
[6] M. Mehring, J.S. Waugh, Magic-angle NMR experiments in solids, Phys. Rev. B 5 (1972) 3459.
[7] B.J. Van Rossum, H. Förster, H.J.M. De Groot, High-field and high-speed CP-MAS ^{13}C NMR heteronuclear dipolar-correlation spectroscopy of solids with frequency-switched Lee–Goldburg homonuclear decoupling, J. Magn. Reson. 124 (1997) 516.
[8] M.H. Levitt, A.C. Kolbert, A. Bielecki, D.J. Ruben, High resolution ^{1}H NMR in solids with frequency-switched multiple pulse sequences, Solid State NMR 2 (1993) 151.
[9] E. Vinogradov, P.K. Madhu, S. Vega, High-resolution proton solid-state NMR spectroscopy by phase-modulated Lee–Goldburg experiment, Chem. Phys. Lett. 314 (1999) 443–450.
[10] A. Ramamoorthy, C.H. Wu, S.J. Opella, Resolved two-dimensional anisotropic-chemical-shift/heteronuclear dipolar coupling powder-pattern spectra by three-dimensional solid-state NMR spectroscopy, J. Magn. Reson. B110 (1999) 102.

[11] C.H. Wu, A. Ramamoorthy, S.J. Opella, High-resolution heteronuclear dipolar solid-state NMR spectroscopy, J. Magn. Reson. A109 (1994) 270.
[12] Katsuyuki Nishimura, Akira Naito, Dramatic reduction of the RF power for attenuation of sample heating in 2D-separated local field solid-state NMR spectroscopy, Chem. Phys. Lett. 402 (2005) 245.
[13] D.K. Lee, T. Narasimhaswamy, A. Ramamoorthy, PITANSEMA, a low-power PISEMA solid state NMR experiment, Chem. Phys. Lett. 399 (2004) 359.
[14] K. Yamamoto, L. Ermakov, D.K. Lee, V.A. Ramamoorthy, PITANSEMA-MAS, a solid state NMR method to measure heteronuclear dipolar couplings under MAS, Chem. Phys. Lett. 408 (2005) 118.
[15] A. Ramamoorthy, Y. Wei, D.K. Lee, PISEMA solid-state NMR spectroscopy, Ann. Rep. NMR Spectrosc. 52 (2004) 1.
[16] G. De Paëpe, D. Sakellariou, P. Hodgkinson, S. Hediger, L. Emsley, Heteronuclear decoupling in NMR of liquid crystals by continuous phase modulation, Chem. Phys. Lett. 368 (2003) 511.
[17] Y. Yu, B.M. Fung, An efficient broadband decoupling sequence for liquid crystals, J. Magn. Reson. 130 (1998) 317.
[18] B.M. Fung, K. Ermolaev, Y. Yu, ^{13}C NMR of liquid crystals with different proton homonuclear dipolar decoupling methods, J. Magn. Reson. 138 (1999) 28.
[19] B.M. Fung, A.K. Khitrin, K. Ermolaev, An improved broadband decoupling sequence for liquid crystals and solids, J. Magn. Reson. 142 (2000) 97.
[20] M. Marjanska, F. Castiglione, J.D. Walls, A. Pines, Measurement of dipolar couplings in partially oriented molecules by local field NMR spectroscopy with low-power decoupling, J. Magn. Reson. 158 (2002) 52.
[21] D.P. Burum, R.R. Ernst, Net polarization transfer via a J-ordered state for signal enhancement of low-sensitivity nuclei, J. Magn. Reson. 39 (1980) 163.
[22] A.E. Bennett, C.M. Rienstra, M. Auger, K.V. Lakshmi, R.G. Griffin, Heteronuclear decoupling in rotating solids, J. Chem. Phys. 103 (1995) 6951.
[23] P. Jensen, H.J. Sass, S. Grzesiek, Improved detection of long-range partially averaged dipolar couplings in weakly aligned samples by Lee–Goldburg decoupling of homonuclear dipolar truncation, J. Biomol. NMR 30 (2004) 443.